Title page

Characteristics of ectopic alveolar basal cells relative to airway basal cells in fibrosis

Sabrina Blumer[1*], Petra Khan PhD[1*], Julien Roux PhD[1,2], Nataliia Artysh[3,4], Linda Plappert[3], Antje Prasse[1,3,4], Katrin E. Hostettler MD PhD[1#].

[1] Department of Biomedicine and Clinics of Respiratory Medicine, University Hospital Basel, University of Basel, Basel 4031, Switzerland;

[2] Swiss Institute of Bioinformatics, Basel, Switzerland;

[3] Fraunhofer Institute for Toxicology and Experimental Medicine, Hannover 30625, Germany;

[4] Hannover Medical School, Department of Pulmonology & Infectious diseases, Hannover, Germany;

*Both authors equally contributed to this manuscript

[#]**Corresponding author:** Katrin E. Hostettler, Prof., Department of Biomedicine, University Hospital Basel, Hebelstrasse 20, 4031 Basel, Switzerland; E-mail: Katrin.Hostettler@usb.ch

Take home message: Alveolar and airway basal cells differ in their transcriptomes and in their capacities to form and to differentiate in organoids, although with no indication of an AT2 cell origin.

ABSTRACT

Rationale: Basal cells (BC) appear ectopically within the lung parenchyma of interstitial lung disease (ILD) patients, potentially through migration of airway BC or though trans-differentiation of alveolar epithelial type 2 (AT2) cells. The exact origin and function of these ectopic alveolar BC remains elusive. By comparing ectopic alveolar to “classical” airway BC, we aimed to get a better understanding of the origin and characteristics of alveolar BC in ILD. **Methods:** Alveolar and airway BC were isolated from transbronchial and airway mucosal biopsies, respectively, from the same ILD patients and expanded in culture. Samples were analyzed by single cell RNA sequencing (scRNA-seq), TaqMan RT-PCR, and immunochemistry. **Results:** scRNA-seq analysis revealed several differences in gene expression that suggested a shift to a more mesenchymal-like phenotype and a decrease in keratinization genes in alveolar compared to airway BC. Specific AT2 cell marker genes were not expressed in either BC type. While the morphology, wound repair and proliferation capacities of BC from both origins were not significantly different, alveolar BC formed significantly fewer organoids, expressing more MUC5B. After instillation into bleomycin-injured mice, alveolar and airway BC showed similar engraftment, differentiation capacity and effects on fibrosis. **Conclusion:** Despite similar overall functionality in vitro and after instillation into bleomycin-injured mice, alveolar and airway BC differed in their transcriptomes and in their capacities to form and to differentiate in organoids. Our data provide no evidence to support their potential derivation from AT2 cells.

Keywords: Airway basal cells, alveolar basal cells, interstitial lung diseases, scRNA-seq, organoids, air liquid interface, mouse model

Introduction

In interstitial lung diseases (ILD) basal cells (BC) accumulate within the alveolar space, where they replace resident alveolar epithelial cells and contribute to pathological honeycomb cysts (HC) formation [1-3]. In the healthy lung, alveoli are lined with alveolar epithelial type (AT)1 and 2 cells, whereas BC are restricted to the airways. AT2 cells are critical for alveolar homeostasis through pulmonary surfactant

production and their ability to self-renew and differentiate into AT1 cells [4]. BC maintain airway homeostasis by self-renewal and the differentiation to other airway epithelial cells such as ciliated, or secretory epithelial cells [5].

The origin of ectopic BC in the alveolar space in ILD remains elusive. BC are present throughout the airways all the way to the terminal bronchioles in human [6]. It is therefore possible that alveolar BC derive from migrated airway BC. Alternatively, studies showed the possibility for AT2 cells to trans-differentiate into BC *in vitro* [7, 8], constituting an alternative explanation for the origin of the alveolar BC pool in ILD.

Some studies suggested a beneficial role of the ectopic BC in ILD in regenerating the injured alveolar epithelium through trans-differentiation to AT2 cells in mice [9, 10]. However, other studies did not find evidence for a contribution of ectopic BC to the AT2 cell pool [11, 12], and suggested that ectopic BC could even play a detrimental role because their abundance correlated with increased mortality and HC formation in ILD [3, 13].

By comparing alveolar BC to their airway counterpart after isolating these two respective BC types from ILD patients and expanding them in culture, we aimed to get a better understanding of the origin and disease-specific characteristics of ectopic BC, which may help to further unravel the pathomechanism of fibrotic ILD.

Materials and Methods

Basal cell culture

Alveolar BC were cultured from transbronchial biopsies (TBB) and airway BC from airway mucosal biopsies (MB) [14-16]. Briefly, TBB or airway MB derived from the same ILD patient were placed into plastic dishes containing an epithelial cell-specific growth medium (Cnt-PR-A). After 5-7 days, tissue was removed and the outgrown cells expanded. Experiments were performed with BC from tissue of several different ILD patients as indicated by the n-number. The local ethical committee of the University Hospital, Basel, Switzerland (EKBB05/06) approved the use of human tissue sections and the culture of human primary lung cells. ILD patient

characteristics and material used in this study are outlined in supplement table 1 and 2.

TaqMan RT-PCR, Immunochemistry

TaqMan RT-PCR, immunocytochemistry (ICC)/immunofluorescence (IF), immunohistochemistry (IHC)/IF or hematoxylin and eosin (H&E) stainings were performed as previously described [15-17]. Primers and antibodies are listed in supplement table 2.

Single-cell RNA-sequencing

scRNA-seq was performed on cultured airway and alveolar BC from three different ILD patients (Patient-ID 01, 02, and 03) using the 10X Genomics technology [17]. Detailed scRNA-seq analysis methods can be viewed in supplement document 1.

Air liquid interface (ALI), organoids, proliferation and epithelial wound repair

BC ALI- and organoid culture as well as proliferation and epithelial wound repair assays were performed as previously [16].

Intratracheal administration of human BC into bleomycin-challenged mice

The Hannover Medical School, Germany performed all mouse procedures in accordance with the German law for animal protection and the European Directive 2010/63/EU and an approval by the Lower Saxony State Office for Consumer Protection and Food Safety in Oldenburg/Germany (LAVES); AZ: 33.12-42502-04-15/1896 and AZ: 33.19-42502-04-15/2017), AZ:33.12-42502-04-17/2612). Human alveolar and airway BC were transduced with a lentiviral vector for firefly-luciferase and enhanced green fluorescence protein (eGFP) [13, 16]. NRG mice (n=9) received bleomycin (1.2 mg/kg) intratracheally. After three days, three mice were intratracheally injected with human alveolar BC, and three mice with human airway BC (both at 0.3 X 10^5 cells per mouse). Firefly-luciferase activity was measured as previously described [13, 16]. At day 21, mice were sacrificed and mouse lungs were formalin-fixed and paraffin embedded (FFPE). Fibrosis scoring was performed on lung tissue of mice treated with bleomycin only (n=3), bleomycin + human alveolar (n=3), or + human airway (n=3) BC [18]: 20 non-overlapping 10x fields per sample

were scored as followed: 0 = no fibrosis, 1 = mild thickening of alveolar septa, 2 = <10%-, 3 = 10–20%, 4 = 20–40%-, 5 = 40–60%-, 6 = 60–80%, 7 = >80% fibrotic area or 8 = complete fibrosis. The scores of all fields were then averaged for each sample.

Statistics

Paired or unpaired t-tests were performed using GraphPad Prism software version 9.1.1. p values < 0.05 were considered as statistically significant. Data were presented as mean ± SEM.

Results

BC characteristics

In airway MB, KRT5+/p63+ BC were lining the basement membrane of the airway epithelium, whereas in TBB, they were found scattered within the lung parenchyma (Figure 1 a). Alveolar and airway BC, isolated and cultured as illustrated (Figure 1 b), were indistinguishable by their morphology (Figure 1 c) and expressed similar levels of BC markers (KRT5, KRT14, KRT17, TP63) both at the RNA and protein level (Figure 1 d). Mesenchymal (CDH2)- or secretory epithelial (SCGB1A1) cell markers were absent or expressed at very low levels (Figure 1 d).

BC transcriptome

scRNA-seq was performed on cultured alveolar and airway BC from 3 ILD patients. After quality control and filtering of cells, 34,435 cells were retained (4,500 to 6,975 cells per sample). The major source of variation across single cells was the individual origin of the sample (Donors 1-3), followed by the origin of the BC samples (TBB or airway MB) (Figure 2 a; Supplement figure 1). After removal of these systematic sources of variation, the cells were grouped into 7 different clusters encompassing between 7.6% and 20% of the cells (Figure 2 b). Each cluster was annotated by comparing our cells to published scRNA-seq atlases of the lung (Figure 2 c [19]; Supplement Figure 2 [1, 2, 7, 20-25]): the majority of cells in clusters 2-6 (84 to 97%) showed closest transcriptomic similarities to the BC subset 1 (canonical BC) described in [19]. Most cells (86%) from cluster 7 closely matched to BC subset 2

(cycling BC) [19]. Last, a large fraction (39%) of cells from cluster 1 matched to BC subset 3 (secretory-primed) [19]. This annotation was supported by inspection of the expression of the best markers across clusters (Figure 2 d) and known marker genes (Supplement Figure 3). More specifically, cluster 7 displayed high expression of proliferation genes such as *PTTG1*, *BIRC5*, *HMGB2*, *MIK67*, *CENPF* and *TOP2A* (Figure 2 d). Secretory-primed BC from cluster 1 were enriched with transcripts of members of the serpin family, *KRT16*, or *CSTA* (Figure 2 d). The markers of the other clusters seemed to illustrate a differentiation gradient from cluster 6 to the secretory-primed cluster 1, analogous to previously reported [15]. In particular cells from cluster 6 were enriched with transcripts highly expressed in undifferentiated BC [26] such as *AREG*, *CAV1*, *THBS1*, or *ITGB4*, whereas transcripts indicating BC to secretory epithelial cell differentiation (*CSTA*, *KRT16*, *SERPINB2*) [27] were expressed at low levels. Their expression increased in cluster 3 and 4 and was highest in cluster 1 (Figure 2 d). Despite expressing lower levels of *AREG*, *CAV1*, *THBS1* and *ITGB4* than cluster 6, cluster 2 showed also lower levels of *CSTA*, *KRT16*, *SERPINB2* than cluster 3 and 4. Instead, high levels of expression of several metallothioneins (e.g., *MT1X*, *MT2A*, *MT1E*), *FOS*, *KRT15*, or *AGR2* were observed, which were in part shared with cluster 3 (Figure 2 d). Cluster 5 showed high expression of the mesenchymal markers *FN1* and *VIM* (Figure 2 d), but it was predominantly composed of cells from donor 1 (74% of cells, Supplement figure 1 a). Of note, there was overall no or very low expression of specific AT2 cell markers (e.g., *SFTPA-D*, *ABCA3*) across cells in our dataset (not shown).

Comparing the relative abundance of alveolar compared to airway BC across clusters (excluding cluster 5 including mostly cells from donor 1), we observed a significantly higher abundance of alveolar BC in cluster 2 (FDR=8.6%), along with a reduced abundance of alveolar BC in cluster 4 (FDR=8.6%) and cluster 1 (FDR=21%) (Figure 2 e). These results suggest an enrichment for an altered differentiation trajectory among alveolar BC (cluster 6 to clusters 2 and 3) relative to the “classical” differentiation trajectory (cluster 6 to cluster 4 and then to cluster 1) enriched among airway BC.

Next, we tested for differences in expression state of alveolar compared to airway BC. Testing within each cluster separately allowed us to account for the above-

described differences in abundance, while the paired design allowed us to account for donor-specific effects. At an FDR of 1%, there were in total 40 genes significantly up or down-regulated in alveolar compared to airway BC in at least one of the clusters (Figure 3 a). Cluster 2 and 6 yielded the highest amount of differentially expressed genes (Figure 3 b; differential expression in other clusters is shown in Supplement Figure 4). Genes involved in response to hypoxia (*PLIN2*, *S100A4*), KRAS activation/mutation (*LMO3*, *IL33*), ECM organization (*SPOCK3*, *MXRA7*), as well as genes involved in glycolysis (*EGLN3*) were up-regulated in alveolar BC, whereas genes involved in interferon response (*IFI27*, *HLA-DRB1*, *BST2*) were down-regulated. Interestingly, although not significant, the BC marker genes *KRT5*, *KRT14, KRT17* and *TP63* were all down-regulated (Supplement Figure 3), whereas *KRT15* and *KRT19* were up-regulated, along with mesenchymal markers such as *FN1*, *COL1A1* or *VIM*.

Functional enrichment analysis using the MSigDB Hallmark pathways (Figure 3 c for clusters 2 and 6; Supplement Figure 5 for clusters 1, 3, 4 and 7) showed that pathways related to hypoxia, glycolysis, angiogenesis, KRAS signaling, and epithelial to mesenchymal transition (EMT) were up-regulated in alveolar BC. Furthermore, Reactome pathway analysis revealed an up-regulation of pathways such as “ECM organization”, “collagen formation”, “collagen biosynthesis and modifying enzymes”, or “activation of matrix metalloproteinases” in alveolar BC (Supplement Figure 6). In line with the above-described trend of keratin genes, the pathway “Keratinization” was significantly down-regulated in alveolar BC in cluster 1, 6, and 7 (Supplement Figure 6).

The differential expression of selected genes was validated in BC from donor 1-3 and three additional donors by TaqMan RT-PCR, confirming the up-regulation of *LMO3*, *S100A4*, *SPOCK3*, *HNMT* and down-regulation of *IFI27*, *BST2* in alveolar relative to airway BC (Figure 3 d).

BC proliferation and wound healing capacities

Alveolar and airway BC numbers significantly increased between 0-48 h (Figure 4 a) and closed a scratch after 6 hours (Figure 4 b) with no difference in cell growth rate (Figure 4 a) or wound healing capacity (Figure 4 b) between alveolar and airway BC.

BC differentiation capacities

Alveolar and airway BC cultured on an ALI (Figure 5 a) differentiated to secretory and ciliated epithelial cells, reflected by a significant increase of secretory (*SCGB1A1*, *MUC5AC*, *MUC5B)* and ciliated (*FOXJ1)* epithelial cell marker expression levels between day 0 and 23 (Figure 5 b). Marker expression levels did not significantly differ between alveolar and airway BC at day 0 or 23 (Figure 5 b). At the protein level, BC did not express AcTub (ciliated epithelial cell marker), MUC5AC, nor SCGB1A1 at day 0 (Figure 4 c), while after 23 days these markers were detected in alveolar and airway BC on PFA-fixed (Figure 5 c) and/or cryo-sectioned (Figure 5 d) ALI membranes.

BC cultured in Matrigel (Figure 6 a) formed organoids (>50µm diameter) after 7 days, which grew in size and number over a period of 21 days (Figure 6 b). After 20 days, alveolar BC formed between 45 and 138 organoids/mm^3, significantly fewer than the 63 to 162 organoids/mm^3 formed by airway BC (Figure 6 c). The size of alveolar (66-122 µm) and airway (73-105 µm) BC-derived organoids was not significantly different (Figure 6 c). After 21 days, cells in alveolar and airway BC-derived organoids expressed similar RNA levels of *TP63*, *KRT5*, *KRT17*, *SCGB1A1*, and *MUC5AC. MUC5B* levels were significantly higher in alveolar BC-derived organoids and FOXJ1 levels showed a non-significant upward trend (Figure 6 d). Marker protein levels were expressed in both alveolar and airway BC, with several cells still expressing basal cell markers (KRT5, p63, KRT17). Differentiated cells primarily expressed MUC5AC, and/or MUC5B, while SCGB1A1 or AcTub proteins were detected in only a view cells (Figure 6 d).

Human BC in bleomycin-challenged mice

Mice were treated as outlined in figure 7 a. BC engrafted and proliferated, which was determined by increasing luciferase expression (Figure 7 b). Bleomycin induced mild fibrotic changes in the mouse lungs, which were slightly increased when alveolar or airway BC were injected (Figure 7 c), but according to fibrosis scores the increase was not significant (Figure 7 c). Co-stainings with human-specific HNA and basal- (KRT5, KRT17), secretory- (MUC5AC, MUC5B, SCGB1A1), or ciliated (AcTub) epithelial cell markers, revealed that human BC maintained their BC identity or

differentiated to MUC5AC+, MUC5B+, or SCGB1A1+ cells in mouse lungs (Figure 7 d). We did not observe differences in fibrosis scores or differentiation capacity within mouse lung tissue, which were injected with either human alveolar or airway BC (Figure 7 c, d).

Discussion

To investigate the origin and characteristics of ectopic alveolar BC in ILD, we made use of a previously established *in vitro* BC culture method [16] allowing us to isolate and expand alveolar and airway BC from the same ILD patients in sufficient numbers. Our data show that BC from the different origins display similar morphology, proliferation and wound healing capacities *in vitro,* as well as comparable engraftment and differentiation abilities when instilled into bleomycin-challenged mice. Despite many similarities, cultured alveolar and airway BC significantly differed in their transcriptomes, and in their potential to form and to differentiate in organoids, although with no indication of an AT2 cell origin.

Transcriptomic differences between alveolar and airway BC included an up-regulation of genes associated with fibrosis-related pathways such as hypoxia, glycolysis, or KRAS signalling in alveolar BC. Hypoxia is increased in fibrotic areas of the ILD lung [28-30], and cellular glycolysis [31] and KRAS signalling [32] are activated under hypoxic conditions. Ectopic BC specifically accumulate in hypoxic regions of the ILD lung parenchyma [28] and were thus likely imprinted by their hypoxic *in vivo* microenvironment. Whether these transcriptomic differences result in altered cellular functions remains to be determined in future studies.

BC in the healthy airways are a heterogeneous cell population, including canonical, proliferating and secretory-primed BC subsets [27]. Both our cultured alveolar and airway BC included cells with close transcriptomic similarity to these BC subsets, secretory-primed BC likely arising through spontaneous BC differentiation in culture, following a clear and previously described differentiation gradient [17]. Interestingly, we observed differences in relative abundance between alveolar and airway BC along this differentiation path, leading to a lower amount of secretory-primed alveolar compared to airway BC. Along the differentiation path, a subpopulation showing

enrichment for several metallothioneins (MTs), FOS, AGR2 or KRT15 was enriched in alveolar BC. This may indicate a slightly altered differentiation path in alveolar BC, resulting in less secretory-primed BC and could be in line with previous studies, showing disturbed cell differentiation with an accumulation of disease-specific intermediate cell types such as the aberrant basaloid cells in ILD lungs [1, 2]. Interestingly, alveolar BC showed a trend towards reduced expression of BC markers and keratinization genes and increased expression of EMT genes and mesenchymal markers, although to a lesser extent than the aberrant basaloid cells [1, 2]. Furthermore, the genes up-regulated in the altered differentiation path were shown to be associated with cancer (MTs [33], FOS [34], AGR2 [35] or KRT15 [36]), which potentially indicates a contribution of ectopic BC to developing lung carcinoma [37], a risk that is increased in IPF [38]. However, these conclusions are speculative and would need rigorous assessment in dedicated studies. Differences in BC subtype composition between alveolar and airway BC populations may also account for the reduced organoid formation capacity of the alveolar BC population, which possibly contains fewer cells with organoid-forming potential.

Ectopic BC lining HC in the IPF parenchyma appear to preferentially differentiate to MUC5B rather than MUC5AC-expressing cells [39]. Here, we demonstrated that both alveolar and airway BC differentiate to MUC5B and MUC5AC-expressing cells when cultured under identical conditions. However interestingly, cultured alveolar BC maintained a significantly higher tendency to differentiate to MUC5B-expressing cells in organoids. This suggests that both the cellular microenvironment and intrinsic cell-specific properties determine BC fate decision.

Human fibrotic BC instilled into mice have previously been shown to aggravate bleomycin-induced fibrosis [13] and to form HC-like structures within the mouse parenchyma [13, 16]. In this study, we confirmed this trend towards increased fibrosis after instillation of BC in the bleomycin-challenged mouse lung as well as their differentiation to secretory epithelial cells. However, we did not observe differences in the mediated effects of BC from the two origins. Of note, the small sample size of this experiment may limit the robustness of the results and needs to be increased in future studies.

Our dataset was not conclusive regarding alveolar BC origin. Human AT2 cells trans-differentiate to BC through intermediate cells, co-expressing varying levels of AT2 cell- and BC marker genes *in vitro* [7]. To determine, if our cultured alveolar BC could originate from AT2 cells, we compared BC and AT2 cell marker gene expression in alveolar versus airway BC. scRNA-seq analysis revealed an overall trend, although not significant, towards reduced BC marker gene expression in alveolar BC, which was, however, not accompanied with expression of specific AT2 cell marker genes. This observation tends to favour the hypothesis that the source of our cultured alveolar BC would be migrating airway BC. However, it is also possible that alveolar BC could have fully lost AT2 cell traits after trans-differentiation in the lung, or later after expanding them in culture. Furthermore, it is also possible that our cell culture method introduce a selection bias by favouring the outgrowth of cells closely related to classic BC, but not that of intermediate cell types.

Acknowledgments

The authors acknowledge the microscopy core facility at the Department of Biomedicine in Basel for their support and assistance in ICC/IF, IHC/IF image acquisition and the sciCORE (http://scicore.unibas.ch/) scientific computing center at the University of Basel for performing calculations.

Author Contributions

SB: Cell culture of human primary lung cells, ALI and organoid processing, ICC/IF, IHC/IF, image acquisition and image quantification in cultured cells, human IPF- and mouse tissue slides, immunoblotting, PCR, proliferation assay, scratch assay, data analysis and interpretation; **PK:** Conception and design of the study, cell culture of human primary lung cells, PCR, data analysis and interpretation, writing the manuscript; **JR:** Data analysis and interpretation of scRNA-seq data, revision and editing of the manuscript for important intellectual content; **NA:** bleomycin-mouse model, data analysis and interpretation, revision and editing of the manuscript for important intellectual content; **LP:** bleomycin-mouse model, data analysis and interpretation, revision and editing of the manuscript for important intellectual content;

AP: bleomycin-mouse model, data analysis and interpretation, revision and editing of the manuscript for important intellectual content; **KEH:** Conception and design of the study, data analysis and interpretation, revision and editing of the manuscript for important intellectual content.

Funding

This study was supported by a project grant (310030_192536) by the Swiss National Research Foundation.

Conflict of interest

The authors have declared that no conflict of interest exists.

Data availability

The processed scRNA-seq dataset (the accession is GSE270495) can be viewed on the gene expression omnibus database (GEO).

References

1. Adams TS, Schupp JC, Poli S, et al. Single-cell RNA-seq reveals ectopic and aberrant lung-resident cell populations in idiopathic pulmonary fibrosis. Science Advances. 2020;6(28):eaba1983.
2. Habermann AC, Gutierrez AJ, Bui LT, et al. Single-cell RNA sequencing reveals profibrotic roles of distinct epithelial and mesenchymal lineages in pulmonary fibrosis. Science Advances. 2020;6(28):eaba1972.
3. Prasse A, Binder H, Schupp JC, et al. BAL Cell Gene Expression Is Indicative of Outcome and Airway Basal Cell Involvement in Idiopathic Pulmonary Fibrosis. Am J Respir Crit Care Med. 2019;199(5):622-630.
4. Barkauskas CE, Cronce MJ, Rackley CR, et al. Type 2 alveolar cells are stem cells in adult lung. J Clin Invest. 2013;123(7):3025-3036.
5. Rock JR, Onaitis MW, Rawlins EL, et al. Basal cells as stem cells of the mouse trachea and human airway epithelium. Proc Natl Acad Sci U S A. 2009;106(31):12771-12775.
6. Basil MC, Morrisey EE. Lung regeneration: a tale of mice and men. Semin Cell Dev Biol. 2020;100:88-100.
7. Kathiriya JJ, Wang C, Zhou M, et al. Human alveolar type 2 epithelium transdifferentiates into metaplastic KRT5(+) basal cells. Nat Cell Biol. 2022;24(1):10-23.
8. Cai XT, Jia M, Heigl T, et al. IL-4-induced SOX9 confers lineage plasticity to aged adult lung stem cells. Cell Reports. 2024;43(8).
9. Kumar PA, Hu Y, Yamamoto Y, et al. Distal airway stem cells yield alveoli in vitro and during lung regeneration following H1N1 influenza infection. Cell. 2011;147(3):525-538.
10. Yuan T, Volckaert T, Redente EF, et al. FGF10-FGFR2B Signaling Generates Basal Cells and Drives Alveolar Epithelial Regeneration by Bronchial Epithelial Stem Cells after Lung Injury. Stem Cell Reports. 2019;12(5):1041-1055.

405 11. Kanegai CM, Xi Y, Donne ML, et al. Persistent Pathology in Influenza-Infected Mouse
406 Lungs. Am J Respir Cell Mol Biol. 2016;55(4):613-615.
407 12. Ray S, Chiba N, Yao C, et al. Rare SOX2(+) Airway Progenitor Cells Generate KRT5(+)
408 Cells that Repopulate Damaged Alveolar Parenchyma following Influenza Virus Infection.
409 Stem Cell Reports. 2016;7(5):817-825.
410 13. Jaeger B, Schupp JC, Plappert L, et al. Airway basal cells show a dedifferentiated
411 KRT17(high)Phenotype and promote fibrosis in idiopathic pulmonary fibrosis. Nat Commun.
412 2022;13(1):5637.
413 14. Hostettler KE, Gazdhar A, Khan P, et al. Multipotent mesenchymal stem cells in lung
414 fibrosis. PLoS One. 2017;12(8):e0181946.
415 15. Khan P, Fytianos K, Blumer S, et al. Basal-Like Cell-Conditioned Medium Exerts Anti-
416 Fibrotic Effects In Vitro and In Vivo. Frontiers in Bioengineering and Biotechnology. 2022;10.
417 16. Blumer S, Khan P, Artysh N, et al. The use of cultured human alveolar basal cells to
418 mimic honeycomb formation in idiopathic pulmonary fibrosis. Respir Res. 2024;25(1):26.
419 17. Khan P, Roux J, Blumer S, et al. Alveolar Basal Cells Differentiate towards Secretory
420 Epithelial- and Aberrant Basaloid-like Cells In Vitro. Cells. 2022;11(11).
421 18. Ashcroft T, Simpson JM, Timbrell V. Simple method of estimating severity of
422 pulmonary fibrosis on a numerical scale. J Clin Pathol. 1988;41(4):467-470.
423 19. Carraro G, Langerman J, Sabri S, et al. Transcriptional analysis of cystic fibrosis
424 airways at single-cell resolution reveals altered epithelial cell states and composition. Nat
425 Med. 2021;27(5):806-814.
426 20. Reyfman PA, Walter JM, Joshi N, et al. Single-Cell Transcriptomic Analysis of Human
427 Lung Provides Insights into the Pathobiology of Pulmonary Fibrosis. Am J Respir Crit Care
428 Med. 2019;199(12):1517-1536.
429 21. Kadur Lakshminarasimha Murthy P, Sontake V, Tata A, et al. Human distal lung maps
430 and lineage hierarchies reveal a bipotent progenitor. Nature. 2022;604(7904):111-119.
431 22. Deprez M, Zaragosi LE, Truchi M, et al. A Single-Cell Atlas of the Human Healthy
432 Airways. Am J Respir Crit Care Med. 2020;202(12):1636-1645.
433 23. Travaglini KJ, Nabhan AN, Penland L, et al. A molecular cell atlas of the human lung
434 from single-cell RNA sequencing. Nature. 2020;587(7835):619-625.
435 24. Strunz M, Simon LM, Ansari M, et al. Alveolar regeneration through a Krt8+
436 transitional stem cell state that persists in human lung fibrosis. Nature Communications.
437 2020;11(1):3559.
438 25. Sikkema L, Ramírez-Suástegui C, Strobl DC, et al. An integrated cell atlas of the lung
439 in health and disease. Nat Med. 2023;29(6):1563-1577.
440 26. Hackett NR, Shaykhiev R, Walters MS, et al. The human airway epithelial basal cell
441 transcriptome. PLoS One. 2011;6(5):e18378.
442 27. Carraro G, Mulay A, Yao C, et al. Single-Cell Reconstruction of Human Basal Cell
443 Diversity in Normal and Idiopathic Pulmonary Fibrosis Lungs. Am J Respir Crit Care Med.
444 2020;202(11):1540-1550.
445 28. Xi Y, Kim T, Brumwell AN, et al. Local lung hypoxia determines epithelial fate
446 decisions during alveolar regeneration. Nat Cell Biol. 2017;19(8):904-914.
447 29. Bodempudi V, Hergert P, Smith K, et al. miR-210 promotes IPF fibroblast proliferation
448 in response to hypoxia. Am J Physiol Lung Cell Mol Physiol. 2014;307(4):L283-294.
449 30. Tzouvelekis A, Harokopos V, Paparountas T, et al. Comparative expression profiling in
450 pulmonary fibrosis suggests a role of hypoxia-inducible factor-1alpha in disease
451 pathogenesis. Am J Respir Crit Care Med. 2007;176(11):1108-1119.

31. Kierans SJ, Taylor CT. Regulation of glycolysis by the hypoxia-inducible factor (HIF): implications for cellular physiology. J Physiol. 2021;599(1):23-37.
32. Zeng M, Kikuchi H, Pino MS, et al. Hypoxia activates the K-ras proto-oncogene to stimulate angiogenesis and inhibit apoptosis in colon cancer cells. PLoS One. 2010;5(6):e10966.
33. Si M, Lang J. The roles of metallothioneins in carcinogenesis. J Hematol Oncol. 2018;11(1):107.
34. Kuonen F, Li NY, Haensel D, et al. c-FOS drives reversible basal to squamous cell carcinoma transition. Cell Rep. 2021;37(1):109774.
35. Moidu NA, NS AR, Syafruddin SE, et al. Secretion of pro-oncogenic AGR2 protein in cancer. Heliyon. 2020;6(9):e05000.
36. Chen W, Miao C. KRT15 promotes colorectal cancer cell migration and invasion through β-catenin/MMP-7 signaling pathway. Med Oncol. 2022;39(5):68.
37. Königshoff M. Lung cancer in pulmonary fibrosis: tales of epithelial cell plasticity. Respiration. 2011;81(5):353-358.
38. Stella GM, D'Agnano V, Piloni D, et al. The oncogenic landscape of the idiopathic pulmonary fibrosis: a narrative review. Transl Lung Cancer Res. 2022;11(3):472-496.
39. Plantier L, Crestani B, Wert SE, et al. Ectopic respiratory epithelial cell differentiation in bronchiolised distal airspaces in idiopathic pulmonary fibrosis. Thorax. 2011;66(8):651-657.

Figure legends

Figure 1: Cultured alveolar and airway BC do not differ in their morphology or BC marker expression. KRT5+ and TP63+ BC in formalin fixed paraffin embedded transbronchial biopsies or airway mucosal biopsies of the same ILD patient (n=5) (a). To culture alveolar or airway BC, tissue specimens were placed in cell culture dishes containing Cnt-PR-A as illustrated in b. Representative phase contrast images showing the morphology of confluent alveolar or airway BC (n=5) (c). RNA expression of KRT5, KRT14, KRT17, TP63, CDH2 or SCGB1A1 (n=6; paired t-test, ns indicates not significant) and representative IF stainings for KRT5/p63, KRT17/KRT14, CDH2, SCGB1A1 KRT5/TP63 (n=3) (d) in cultured alveolar and airway BC.

Figure 2: Alveolar and airway BC differ in their transcriptome. T-SNE plot (uncorrected data) showing cultured alveolar and airway BC derived from donor 1-3 (a). T-SNE (after MNN correction) showing the separation of cells into 7 clusters (b). T-SNE showing the best-matching reference label in the transcriptome comparison to a publicly available scRNA-seq dataset [41] (c). Heatmap of the relative

expression across clusters, donors, and sample location of the strongest cluster-specific genes. The log- normalized expression levels were averaged across cells from the same cluster, donor, and sample location, corrected for donor-specific effects to mirror the MNN correction performed before clustering and the inclusion of donor as a covariate in the differential expression analysis, and averaged values were then centered and scaled per gene. Marker genes are highlighted in bold (d). Proportion of alveolar and airway BC across donors in clusters 1, 2, 3, 4, 6, and 7 (e).

Figure 3: Differential genes and pathways in alveolar versus airway BC. Heatmap showing the differential expressed genes in alveolar versus airway BC across all tested clusters. The plotted relative expression values were calculated similarly to Figure 2D. Annotation colors for rows indicate in which specific cluster each gene was found significantly differentially expressed at an FDR threshold of 1% (a). Volcano plots showing the differential expression analysis results between alveolar and airway BC in cluster 2 and cluster 6 (b). Genes colored (beige=decreased, and blue=increased in alveolar BC relative to airway BC) are significant at an FDR threshold of 1% (b). Functional enrichment analysis amongst differentially expressed genes in cluster 2 and cluster 6 (c) using MSigDB Hallmark gene sets. Six differentially expressed genes (*LMO3*, *S100A4*, *SPOCK3*, *HNMT*, *IFI27*, *BST2*) were selected and analyzed by Taqman RT-qPCR (d). Data points in red represent results from cells derived from donor 1-3. Data points in black were derived from cells of three additional donors (paired t-test, ** indicates $p < 0.01$, * indicates $p < 0.05$).

Figure 4: Alveolar and airway basal cells display similar proliferation and wound healing capacities. Automated cell counts of cultured alveolar and airway BC at 0 and 48 hours (paired t-test, *** indicates $p < 0.001$, * indicates $p < 0.05$) and their growth rate (cell number at day 48 - cell number at day 0) comparing alveolar to airway BC (n=4; paired t-test, ns indicates not significant) (a). Representative phase contrast images and graph displaying alveolar and airway BC wound closure (%) between 0-24 h (mean ± SEM, paired t-test ns indicates not significant) (b).

Figure 5: Alveolar and airway basal cells have similar differentiation capacities. Illustration of alveolar and airway BC ALI culture (a). RNA expression levels (-ΔCt) of KRT5, SCGB1A1, MUC5AC, MUC5B, or FOXJ1 in ALI-cultured alveolar and airway BC (n=4) at day 0 and 23 (paired t-test, **** indicates $p < 0.0001$, *** indicates $p < 0.001$, ** indicates $p < 0.01$, * indicates $p < 0.05$) and comparing their expression in alveolar versus airway BC (paired t-test, ns indicates not significant) (b). When the target genes were expressed at levels too low to be detected after 40 cycles, the missing -ΔCt values were arbitrarily set to -20 (b). Representative ICC/IF images of alveolar and airway BC (n=3) incubated with antibodies detecting acetylated-tubulin (AcTub), MUC5AC or SCGB1A1 at day 0 and 23 (c). Representative images of cryosections incubated with antibodies detecting KRT5, p63, SCGB1A1, KRT17, MUC5AC, MUC5B, or AcTub of ALI-cultured alveolar or airway BC (n=3) at day 23 (d).

Figure 6: Alveolar and airway basal cells form organoids containing basal, secretory- and ciliated epithelial cells. Alveolar and airway BC were resuspended in Matrigel and cultured for 21 days as illustrated (a). Representative phase contrast images of alveolar or airway BC (n=7) organoid formation at day 2, 7, 14, and 21 (b). Number of alveolar and airway BC-derived organoids/mm^3 and the distribution of their diameters (>50µm) after 20 days (n=7; paired t-test, * values ≤ 0.05, ns=not significant) (c). RNA expression levels (-ΔCt) of TP63, KRT5, KRT17, SCGB1A1, MUC5AC, MUC5B, or FOXJ1 in organoids after 21 days (n=4; paired t-test, * values ≤ 0.05, ns=not significant) and representative H&E and ICC/IF images of alveolar or airway BC-derived organoids (n=3) incubated with antibodies detecting KRT17, KRT5, p63, SCGB1A1, AcTub, MUC5AC, or MUC5B (d).

Figure 7: Human alveolar or airway basal cells in bleomycin-challenged mouse lungs. NRG mice were treated with bleomycin (n=3) +/- human alveolar (n=3) or airway (n=3) BC carrying a luciferase encoding vector as illustrated (a). Luciferase expression in mice treated with bleomycin +/- human alveolar or airway BC carrying a luciferase encoding vector and the corresponding bioluminescence measurements at day 4, 11, and 21 (b). Representative images of H&E stainings and fibrosis scores

for mice treated with bleomycin +/- human alveolar or airway BC (unpaired t-test, Bleo versus Bleo+ alveolar or airway BC; paired t-test for Bleo+ alveolar BC versus Bleo+ airway BC) (c). Representative IHC/IF images of mouse lung tissue (mice treated with bleomycin + human alveolar or airway BC) incubated with antibodies detecting human-specific HNA with or without KRT5, KRT17, SCGB1A1, MUC5AC, MUC5B, or AcTub. Nuclei were counter-stained with DAPI. White squares indicate regions imaged at higher magnification (d).

Supplement figure 1: tSNE showing the distribution of alveolar and airway BC from donor 1 (airway BC-green; alveolar BC- grey), donor 2 (airway BC- dark green; alveolar BC- light blue) and donor 3 (airway BC- lilac; alveolar BC-purple) (a). Percentage of scRNA-seq reads originating from mitochondrial genes (b). Number of detected genes across cells (number of genes with at least one UMI count, on a log-scale) (c).

Supplement figure 2: tSNE showing the best matching cell type for each cell from the *SingleR* analysis using as reference the scRNA-seq datasets from Adams et al. [1], Habermann et al. [2], Reyfmann et al. [20], Travaglini et al. [23], Kathiriya et al. [7], Sikkema et al. [25], Murthy et al. [21], Strunz et al. [24] or Deprez et al. [22]. Cell types represented by no more than 5 cells in our dataset were pooled into the category “Others”.

Supplement figure 3: Heatmap of the relative expression across clusters, donors, and sample location of selected marker genes.

Supplement figure 4: Volcano plots showing the differential expression analysis results between alveolar and airway BC in cluster 1 (a), cluster 3 (b), cluster 4 (c), and cluster 7 (d). Genes colored (beige=decreased, and blue=increased in alveolar BC relative to airway BC) are significant at an FDR threshold of 1%.

Supplement figure 5: Functional enrichment analysis amongst differentially expressed genes in cluster 1 (A), cluster 3 (B), cluster 4 (C), and cluster 7 (D) using MSigDB Hallmark gene sets.

Supplement figure 6: Functional enrichment analysis amongst differentially expressed genes in clusters 1-4, cluster 6 and cluster 7 using the MSigDB Reactome gene sets from the C2 collection.

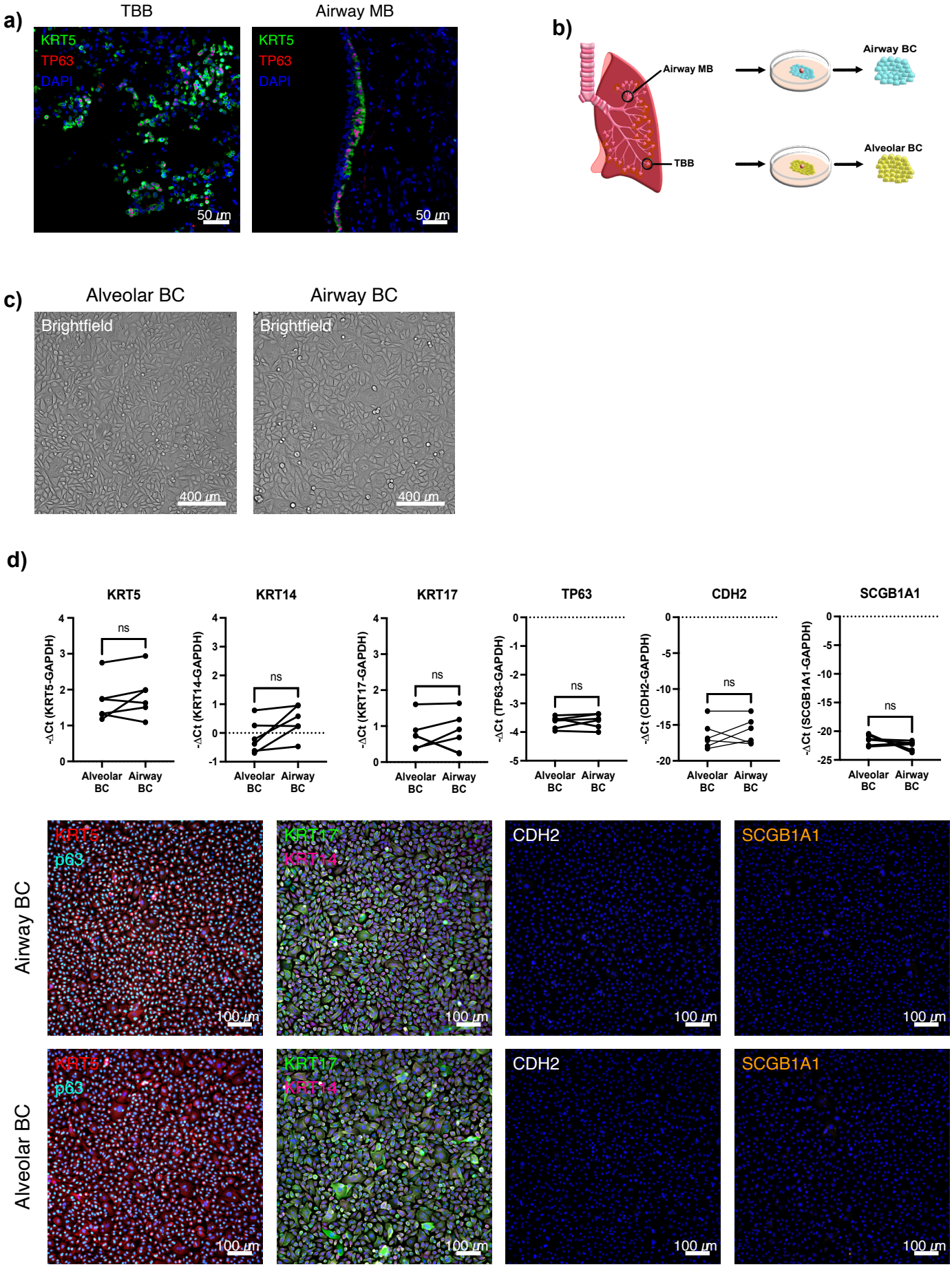
a)
TBB
Airway MB
KRT5
TP63
DAPI
50 µm
b)
Airway MB
TBB
Airway BC
Alveolar BC
c)
Alveolar BC
Airway BC
Brightfield
400 µm
d)
KRT5
KRT14
KRT17
TP63
CDH2
SCGB1A1
-ΔCt (KRT5-GAPDH)
-ΔCt (KRT14-GAPDH)
-ΔCt (KRT17-GAPDH)
-ΔCt (TP63-GAPDH)
-ΔCt (CDH2-GAPDH)
-ΔCt (SCGB1A1-GAPDH)
ns
Alveolar BC
Airway BC
Airway BC
Alveolar BC
p63
100 µm

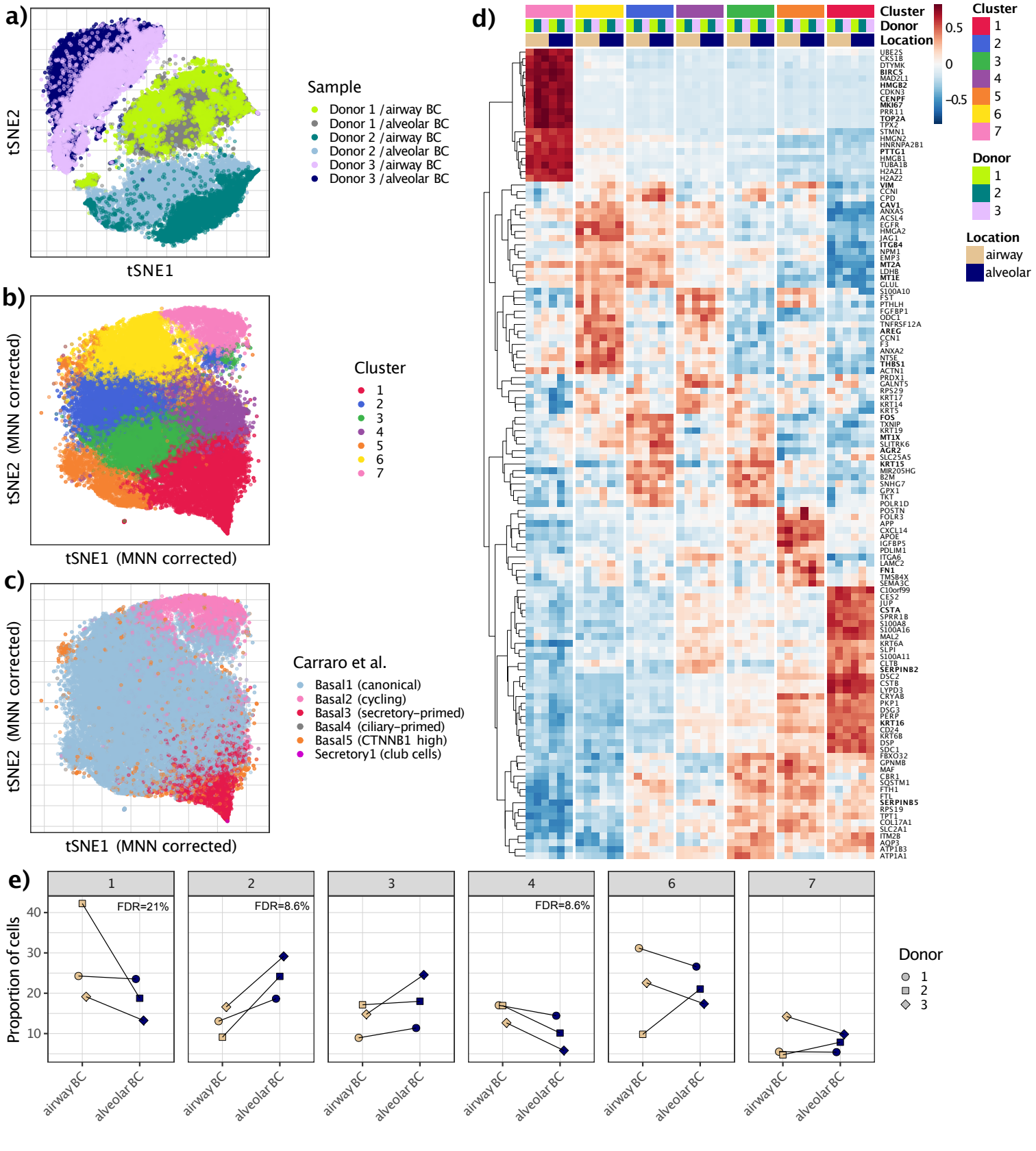
a)
tSNE2
tSNE1
Sample
Donor 1 /airway BC
Donor 1 /alveolar BC
Donor 2 /airway BC
Donor 2 /alveolar BC
Donor 3 /airway BC
Donor 3 /alveolar BC
b)
tSNE2 (MNN corrected)
tSNE1 (MNN corrected)
Cluster
1
2
3
4
5
6
7
c)
tSNE2 (MNN corrected)
tSNE1 (MNN corrected)
Carraro et al.
Basal1 (canonical)
Basal2 (cycling)
Basal3 (secretory-primed)
Basal4 (ciliary-primed)
Basal5 (CTNNB1 high)
Secretory1 (club cells)
d)
Cluster
Donor
Location
0.5
0
−0.5
Cluster
1
2
3
4
5
6
7
Donor
1
2
3
Location
airway
alveolar
UBE2S
CKS1B
DTYMK
BIRC5
MAD2L1
HMGB2
CDKN3
CENPF
MKI67
PRR11
TOP2A
TPX2
STMN1
HMGN2
HNRNPA2B1
PTTG1
HMGB1
TUBA1B
H2AZ1
H2AZ2
VIM
CCNI
CPD
CAV1
ANXA5
ACSL4
EGFR
HMGA2
JAG1
ITGB4
NPM1
EMP3
MT2A
LDHB
MT1E
GLUL
S100A10
FST
PTHLH
FGFBP1
ODC1
TNFRSF12A
AREG
CCN1
F3
ANXA2
NT5E
THBS1
ACTN1
PRDX1
GALNT5
RPS29
KRT17
KRT14
KRT5
FOS
TXNIP
KRT19
MT1X
SLITRK6
AGR2
SLC25A5
KRT15
MIR205HG
B2M
SNHG7
GPX1
TKT
POLR1D
POSTN
FOLR3
APP
CXCL14
APOE
IGFBP5
PDLIM1
ITGA6
LAMC2
FN1
TMSB4X
SEMA3C
C10orf99
CES2
JUP
CSTA
SPRR1B
S100A8
S100A16
MAL2
KRT6A
SLPI
S100A11
CLTB
SERPINB2
DSC2
CSTB
LYPD3
CRYAB
PKP1
DSG3
PERP
KRT16
CD24
KRT6B
DSP
SDC1
FBXO32
GPNMB
MAF
CBR1
SQSTM1
FTH1
FTL
SERPINB5
RPS19
TPT1
COL17A1
SLC2A1
ITM2B
AQP3
ATP1B3
ATP1A1
e)
1
2
3
4
6
7
FDR=21%
FDR=8.6%
FDR=8.6%
Proportion of cells
40
30
20
10
airway BC
alveolar BC
Donor
1
2
3

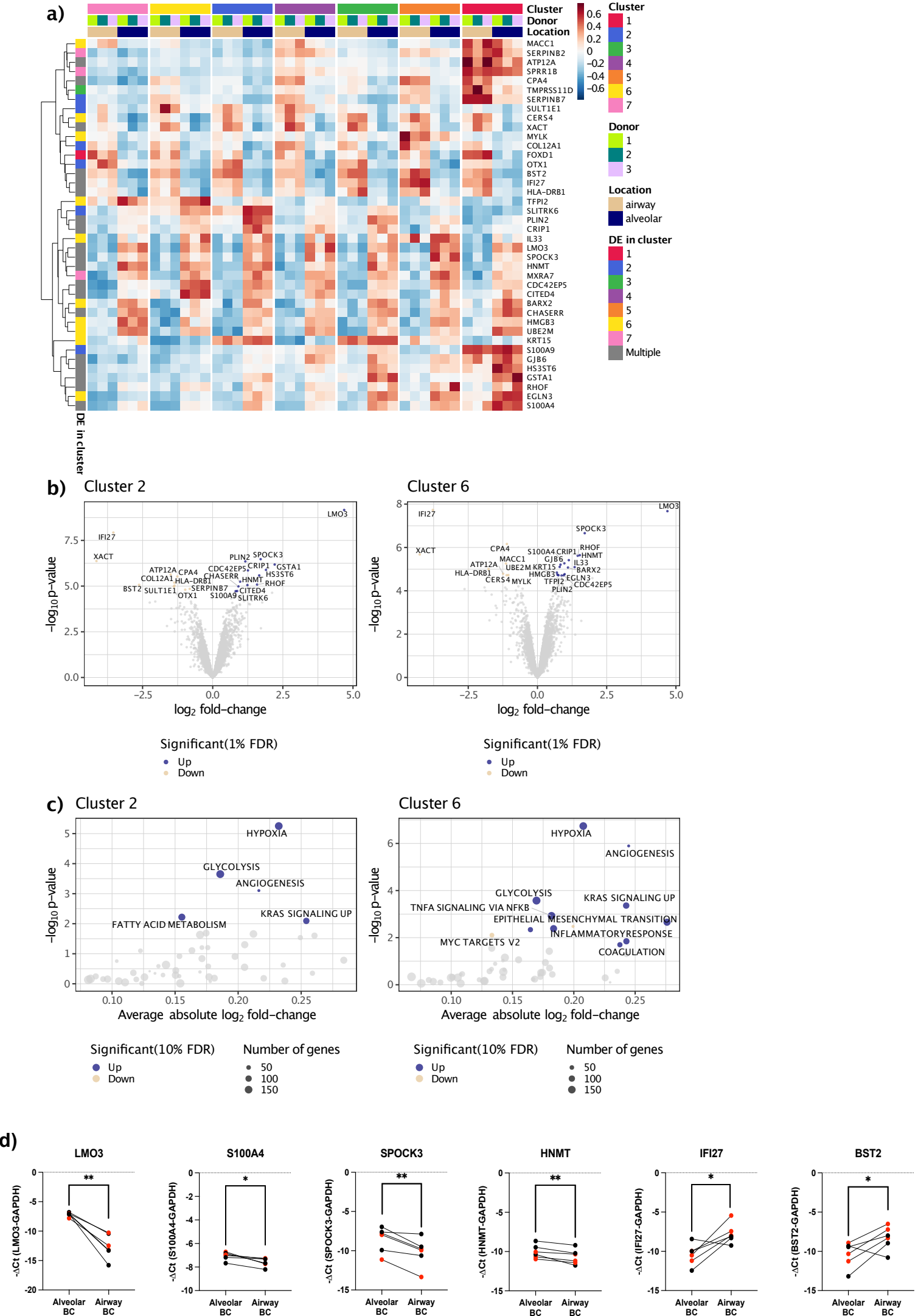
a)
Cluster
Donor
Location
MACC1
SERPINB2
ATP12A
SPRR1B
CPA4
TMPRSS11D
SERPINB7
SULT1E1
CERS4
XACT
MYLK
COL12A1
FOXD1
OTX1
BST2
IFI27
HLA-DRB1
TFPI2
SLITRK6
PLIN2
CRIP1
IL33
LMO3
SPOCK3
HNMT
MXRA7
CDC42EP5
CITED4
BARX2
CHASERR
HMGB3
UBE2M
KRT15
S100A9
GJB6
HS3ST6
GSTA1
RHOF
EGLN3
S100A4
DE in cluster
Cluster
1
2
3
4
5
6
7
Donor
1
2
3
Location
airway
alveolar
DE in cluster
1
2
3
4
5
6
7
Multiple
b)
Cluster 2
Cluster 6
−log10 p−value
log2 fold−change
Significant(1% FDR)
Up
Down
c)
Cluster 2
Cluster 6
HYPOXIA
GLYCOLYSIS
ANGIOGENESIS
KRAS SIGNALING UP
FATTY ACID METABOLISM
TNFA SIGNALING VIA NFKB
EPITHELIAL MESENCHYMAL TRANSITION
INFLAMMATORYRESPONSE
MYC TARGETS V2
COAGULATION
Average absolute log2 fold−change
Significant(10% FDR)
Number of genes
d)
LMO3
S100A4
SPOCK3
HNMT
IFI27
BST2
-ΔCt (LMO3-GAPDH)
-ΔCt (S100A4-GAPDH)
-ΔCt (SPOCK3-GAPDH)
-ΔCt (HNMT-GAPDH)
-ΔCt (IFI27-GAPDH)
-ΔCt (BST2-GAPDH)
Alveolar BC
Airway BC

a)

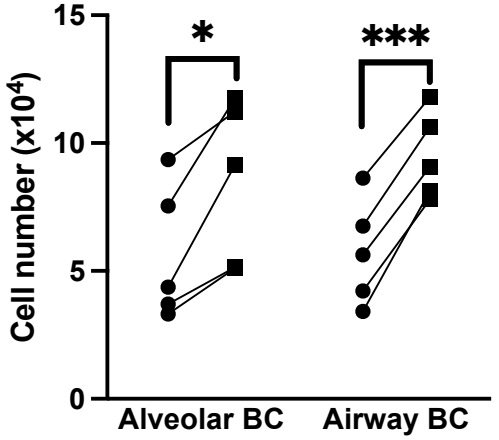
Cell number (x10⁴)
15
10
5
0
*
***
Alveolar BC
Airway BC

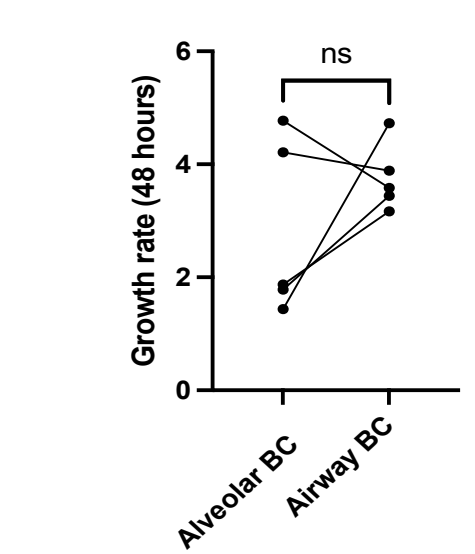
0 hours
48 hours
Growth rate (48 hours)
6
4
2
0
ns
Alveolar BC
Airway BC

b)

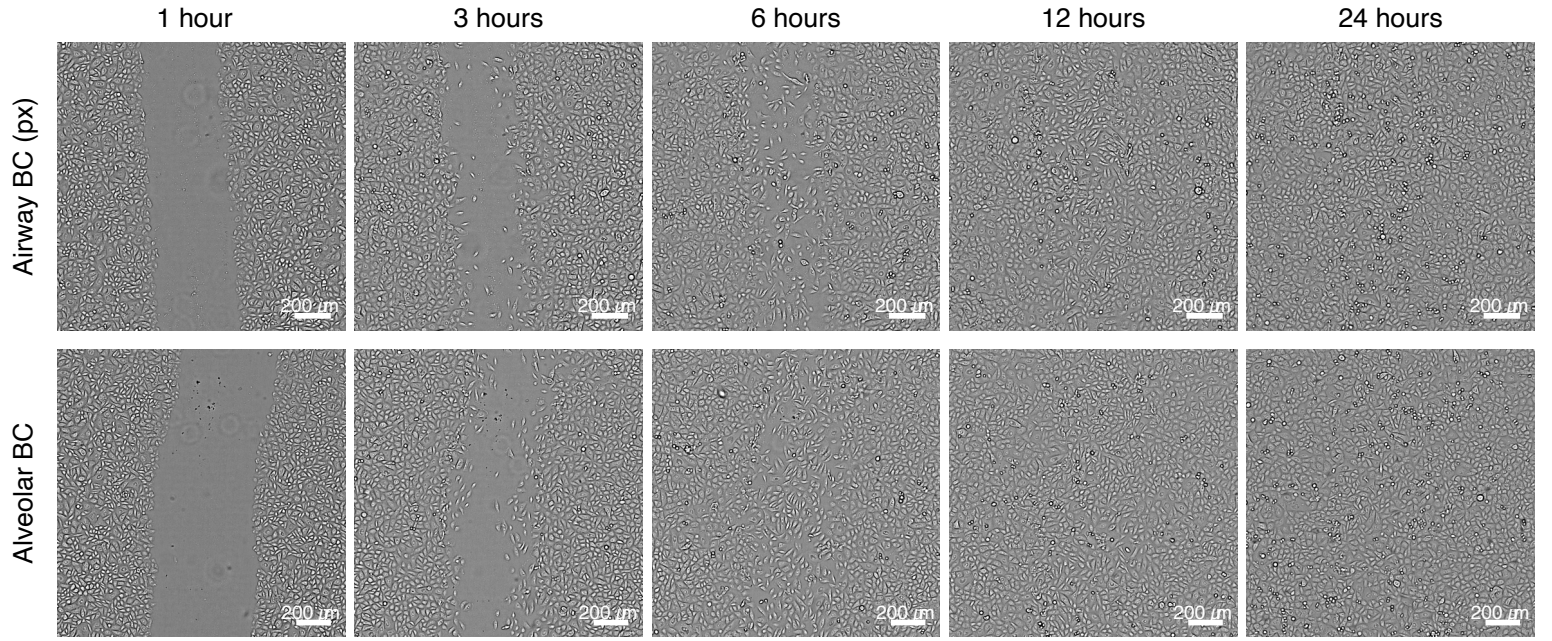
1 hour
3 hours
6 hours
12 hours
24 hours
Airway BC (px)
Alveolar BC
200 µm

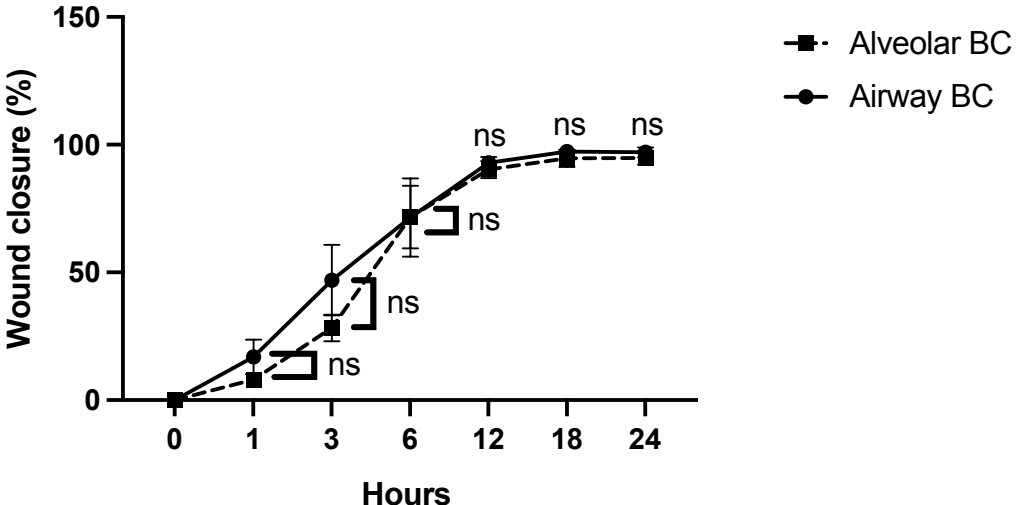
Wound closure (%)
150
100
50
0
0
1
3
6
12
18
24
Hours
ns
Alveolar BC
Airway BC

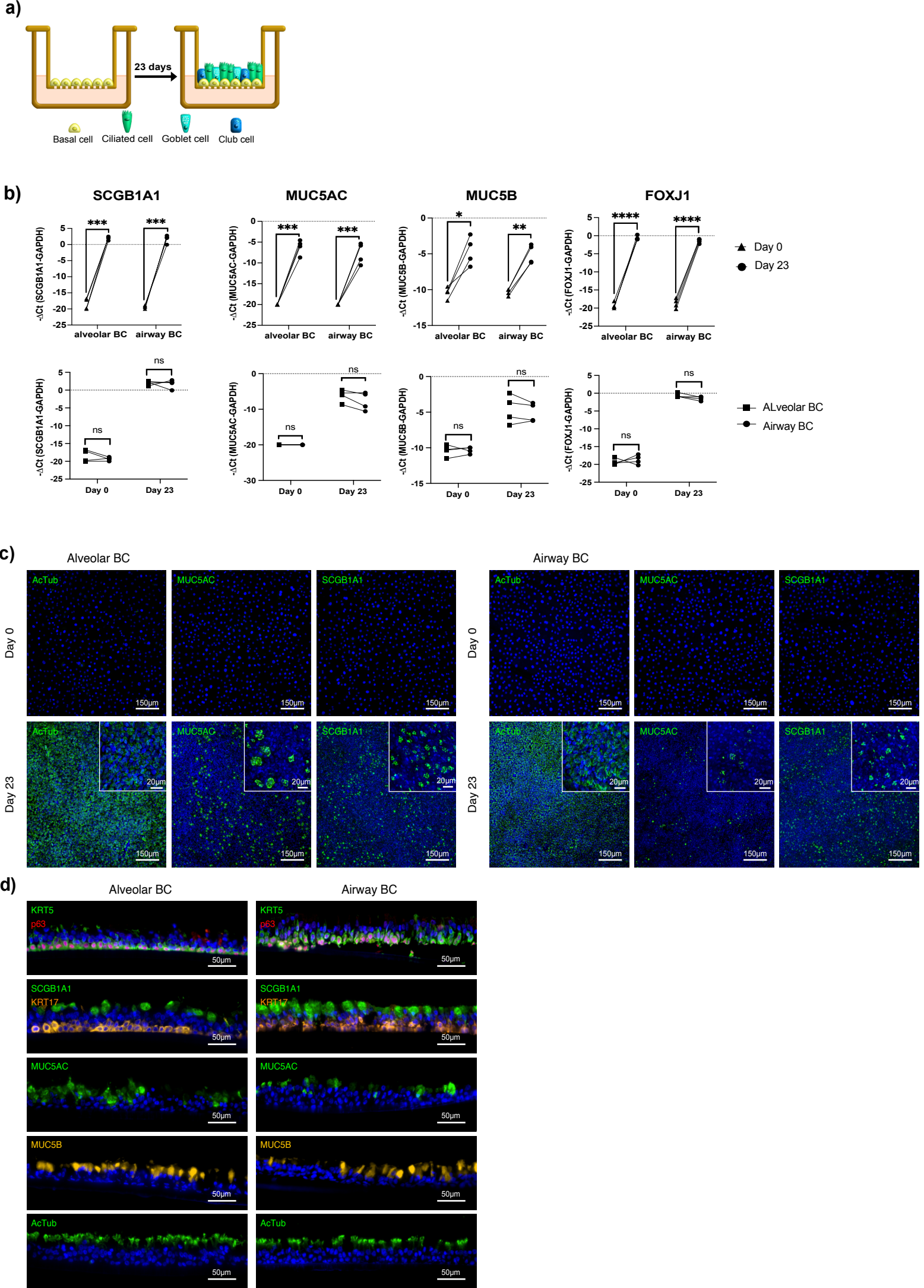
a)
23 days
Basal cell
Ciliated cell
Goblet cell
Club cell
b)
SCGB1A1
MUC5AC
MUC5B
FOXJ1
-ΔCt (SCGB1A1-GAPDH)
-ΔCt (MUC5AC-GAPDH)
-ΔCt (MUC5B-GAPDH)
-ΔCt (FOXJ1-GAPDH)
alveolar BC
airway BC
Day 0
Day 23
ns
ALveolar BC
Airway BC
c)
Alveolar BC
Airway BC
AcTub
MUC5AC
SCGB1A1
150µm
20µm
d)
KRT5
p63
KRT17
50µm

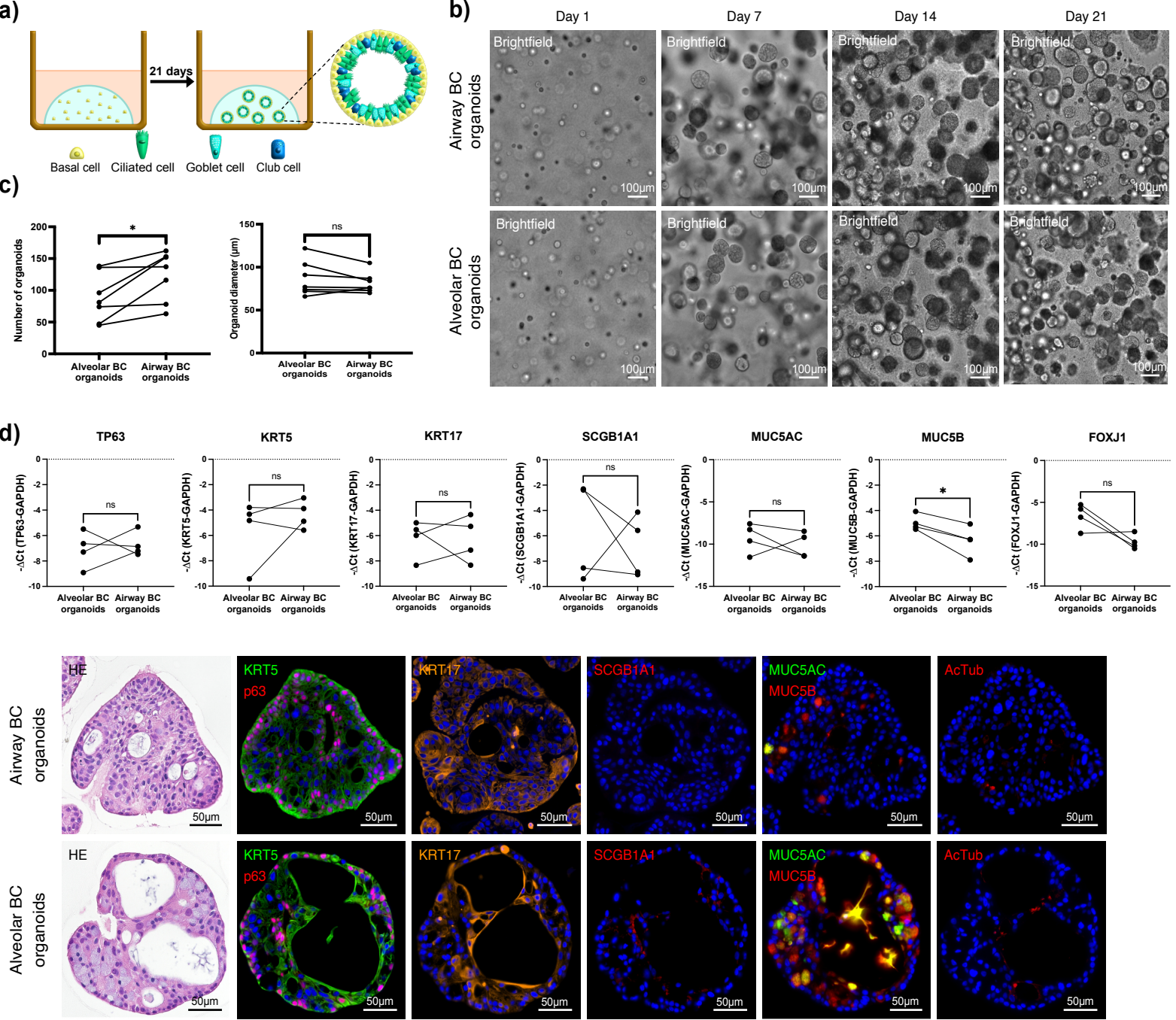
a)
21 days
Basal cell
Ciliated cell
Goblet cell
Club cell
b)
Day 1
Day 7
Day 14
Day 21
Airway BC organoids
Alveolar BC organoids
Brightfield
100µm
c)
Number of organoids
Organoid diameter (µm)
Alveolar BC organoids
Airway BC organoids
*
ns
d)
TP63
KRT5
KRT17
SCGB1A1
MUC5AC
MUC5B
FOXJ1
-ΔCt (TP63-GAPDH)
-ΔCt (KRT5-GAPDH)
-ΔCt (KRT17-GAPDH)
-ΔCt (SCGB1A1-GAPDH)
-ΔCt (MUC5AC-GAPDH)
-ΔCt (MUC5B-GAPDH)
-ΔCt (FOXJ1-GAPDH)
HE
KRT5
p63
KRT17
SCGB1A1
MUC5AC
MUC5B
AcTub
50µm

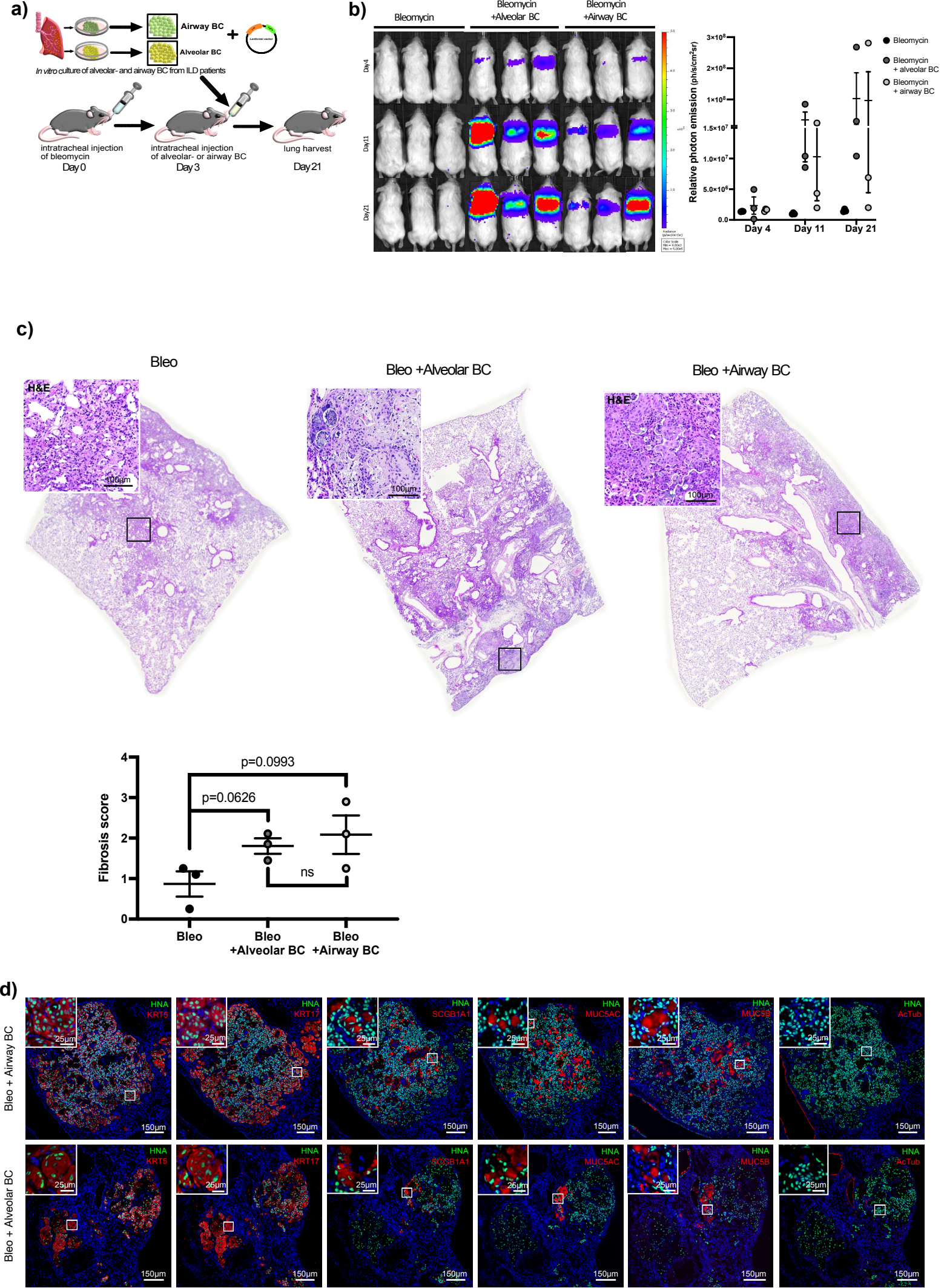
a)
Airway BC
Alveolar BC
In vitro culture of alveolar- and airway BC from ILD patients
intratracheal injection of bleomycin
Day 0
intratracheal injection of alveolar- or airway BC
Day 3
lung harvest
Day 21
b)
Bleomycin
Bleomycin +Alveolar BC
Bleomycin +Airway BC
Day 4
Day 11
Day 21
Relative photon emission (ph/s/cm²sr)
Bleomycin
Bleomycin + alveolar BC
Bleomycin + airway BC
c)
Bleo
Bleo +Alveolar BC
Bleo +Airway BC
H&E
100µm
Fibrosis score
p=0.0993
p=0.0626
ns
Bleo
Bleo +Alveolar BC
Bleo +Airway BC
d)
Bleo + Airway BC
Bleo + Alveolar BC
HNA
KRT5
KRT17
SCGB1A1
MUC5AC
MUC5B
AcTub
25µm
150µm